8-6-2010

An invisible quantum tripwire

Petr M. Anisimov
Louisiana State University

Daniel J. Lum
Louisiana State University

S. Blane McCracken
Louisiana State University

Hwang Lee
Louisiana State University

Jonathan P. Dowling
Louisiana State University

Recommended Citation

Anisimov, P., Lum, D., Blane McCracken, S., Lee, H., & Dowling, J. (2010). An invisible quantum tripwire. *New Journal of Physics, 12* https://doi.org/10.1088/1367-2630/12/8/083012

OPEN ACCESS

An invisible quantum tripwire

New Journal of Physics
The open-access journal for physics

An invisible quantum tripwire

Petr M Anisimov[1], **Daniel J Lum, S Blane McCracken, Hwang Lee and Jonathan P Dowling**

Hearne Institute for Theoretical Physics and Department of Physics and Astronomy, Louisiana State University, Baton Rouge, LA 70803, USA
E-mail: petr@lsu.edu

New Journal of Physics **12** (2010) 083012 (8pp)
Received 26 April 2010
Published 6 August 2010
Online at http://www.njp.org/
doi:10.1088/1367-2630/12/8/083012

Abstract. We present here a quantum tripwire, which is a quantum optical interrogation technique capable of detecting an intrusion with very low probability of the tripwire being revealed to the intruder. Our scheme combines interaction-free measurement (IFM) with the quantum Zeno effect in order to interrogate the presence of the intruder without interaction. The tripwire exploits a curious nonlinear behaviour of the quantum Zeno effect we discovered, which occurs in a lossy system. We also employ a statistical hypothesis testing protocol, allowing us to calculate a confidence level of IFM after a given number of trials. As a result, our quantum intruder alert system is robust against photon loss and dephasing under realistic atmospheric conditions and its design minimizes the probabilities of false positives and false negatives as well as the probability of becoming visible to the intruder.

Contents

1. Introduction 2
2. Interaction-free measurement 2
3. Invisible hypothesis testing 3
4. Invisible tripwire 4
5. Results 6
6. Conclusion 8
Acknowledgments 8
References 8

[1] Author to whom any correspondence should be addressed.

1. Introduction

Interaction-free measurement (IFM) originated with the Elitzur–Vaidman 'Bomb' gedanken experiment that showed that it was possible to detect a single-photon, hair-triggered bomb in an interferometer—without setting it off—by exploiting single-particle interference combined with the presence of quantum 'which-path' information [1]. The original bomb protocol had a success probability of only 25%. (In another 50% of the runs, the bomb was detonated, and in the remaining 25%, no information about the bomb was obtained.) The protocol was improved upon by Kwiat *et al*, who combined lossless IFM with a multi-pass quantum Zeno effect [2]. In our work presented here, we discovered a curious nonlinear behaviour of the photon transmission in a Zeno enhanced but lossy IFM apparatus. This discovery led us to an IFM protocol robust against photon loss and dephasing. In addition, we recast the entire protocol in terms of statistical hypothesis testing, allowing us to quantify the operation of the device as a reliable yet undetectable intruder alert system—the invisible quantum tripwire (IQT).

2. Interaction-free measurement

The Elitzur–Vaidman 'Bomb' gedanken experiment posits that there exists a bomb with a single-photon sensitive detonator and the goal is to optically detect the presence of such a bomb without detonation. In contrast to the expectations of the classical approach, where such a goal could not be reached, quantum optics allows for a solution—measurement without interaction.

This measurement is based on the fascinating property of a single photon to interfere with itself while being indivisible. Imagine a lossless Mach–Zehnder interferometer (MZI) with beam splitters described by a two-mode coupling matrix

$$\hat{U}(\theta_i) = \begin{bmatrix} \cos\theta_i & -\sin\theta_i \\ \sin\theta_i & \cos\theta_i \end{bmatrix}, \tag{1}$$

and the possibility of a photon-sensitive object to be placed in the detection arm (see figure 1). This detection arm stays invisible to the object for as long as a photon has not been absorbed by the object. There are two possible scenarios: the path is blocked or it is clear. If the path is clear, a single photon, after the first beam splitter $\hat{U}(\theta_1)$, can travel both the arms of an interferometer and interfere with itself at the second beam splitter $\hat{U}(\theta_2)$. Under a proper choice of beam splitters, $\theta_1 + \theta_2 = \pi/2$, and a zero phase difference, such an interference will result in zero probability of the photon leaving the MZI in mode A (dark port), that is, $P_0(D) = 0$. If the path is blocked by an object $\hat{O}$, there is definite destruction of the interference as well as the probability of an object absorbing a photon, $P_1(A) = \sin^2\theta_1$. Loss of the photon tells us that an object is there, but this is a measurement with an interaction. Without interference there is non-zero probability of a photon exiting the MZI through the dark port, $P_1(D) = \cos^2\theta_1 \cos^2\theta_2$. Detection of a photon in a dark port constitutes a measurement without an interaction. The efficiency of a given measurement is $\eta = P_1(D)/[P_1(D) + P_1(A)]$, since an object is detected with probability $P_1(D) + P_1(A)$, while detection without interaction is carried out with probability $P_1(D)$. In the presented setup, there is a limit on the highest efficiency $\eta = \cos^2\theta_1/(1 + \cos^2\theta_1) \leqslant 1/2$, which is achieved at the limit where $P_1(D) \to 0$, $P_1(B) \to P_0(B) = 1$ and single trial detection becomes improbable.

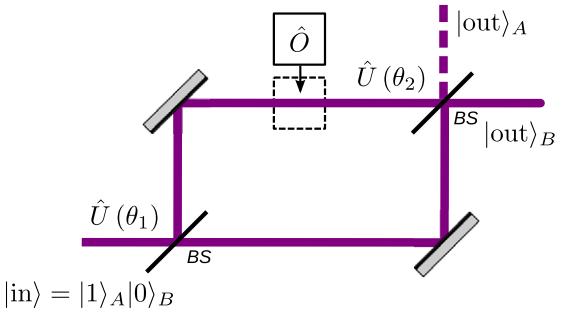

Figure 1. A lossless MZI in a dark port arrangement, $\theta_1 + \theta_2 = \pi/2$, and in a zero phase difference between its arms constitutes a simple IFM setup with efficiency $\eta \leqslant 1/2$. This scheme allows for interaction-free hypothesis testing of a path being blocked (h_1) or clear (h_0).

3. Invisible hypothesis testing

Clearly, these two scenarios correspond to two hypotheses h_1 and h_0 that an IFM apparatus tests for without interaction. These two hypotheses hold equal statistical weight (symmetric testing) and are described by possible outcomes $b = \{A, B, D\}$ and their corresponding probabilities $P_1(b)$ and $P_0(b)$ for the first and second hypotheses, respectively. Due to the probabilistic nature of the outcomes, there is always a chance of a false positive. This error of choice after a single trial is limited by the classical Chernoff bound [3]:

$$P_e \leqslant \frac{1}{2} \min_{s\in[0,1]} \sum_b P_0^s(b) P_1^{1-s}(b). \tag{2}$$

Meanwhile, the classical Chernoff bound on the error of choosing the wrong hypothesis after M trials scales exponentially, $P_e < \frac{1}{2}e^{-MC(P_0,P_1)} \equiv P_e^{\max}$, where $C(P_0, P_1) = -\min_{s\in[0,1]} \ln(\sum_b P_0^s(b) P_1^{1-s}(b))$ is known as the Chernoff distance.

Our IFM apparatus performs interaction-free hypothesis testing based on three possible outcomes: ($b = A$) the probability of absorption because of photon loss or a measurement with an interaction, ($b = D$) the probability of an IFM and ($b = B$) the probability of learning nothing of where the photon exits through the bright port of the interferometer. The importance of no photon loss without an object, $P_0(A) = 0$, and the dark-port condition, $P_0(D) = 0$, becomes now obvious in the light of equation (2). These assumptions ensure that the error of false acceptance comes from the probability of a photon exiting through the bright port in the presence of an object $P_1(B) = \cos^4\theta_1$ and is equal to $P_e = \frac{1}{2}P_1(B)$ due to a 50 : 50 chance of wrongly choosing after such an outcome.

The error of false acceptance in a lossless MZI with a dark port is minimized by an increase of the first beam splitter's reflectance ($\theta_1 \to \pi/2$). It means that all the photons are routed into the detection arm. Hence, interaction with an object becomes unavoidable and the photon path becomes visible. In the opposite case, $\theta_1 \to 0$, the probability of interaction with the object is significantly reduced, at the expense of high statistical error. In order to compensate for the increased statistical error, multiple trials are required. For the photon path to stay invisible to the object, every photon must be received at the output, which happens with the probability $\bar{P}_{\text{vis}} = \exp(-MC_{\text{vis}})$, where the visibility distance, $C_{\text{vis}} = -\ln\cos^2\theta_1$, is introduced

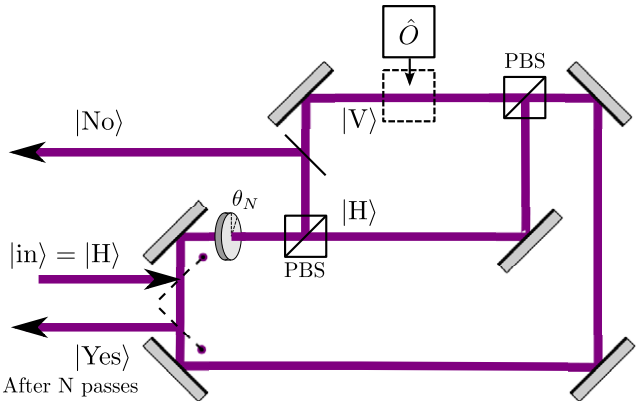

Figure 2. IQT apparatus based on an N-pass IFM in the polarization interferometer. With each pass, the photon's polarization is rotated by an angle θ_N. The presence of an object prevents accumulation of polarization rotation and is similar to the quantum Zeno effect [4, 5]. An additional beam splitter inside the polarization interferometer models unavoidable loss in the arm accessible by the object as well as controlled loss that is adjusted to provide the best performance of the IQT apparatus.

for an easy comparison with the Chernoff distance, $C(P_0, P_1) = -2 \ln \cos^2 \theta_1$. Judging from these distances, it is possible for the detection to be hidden from the object, $\bar{P}_{\text{vis}} \gg 0$, while revealing the presence of the object with a high level of certainty $P_e \to 0$. Sadly, any deviation from the ideal setup—such as loss, phase shifts or non-perfect dark port arrangement—makes the Chernoff and visibility distances comparable, thus effectively preventing the invisibility of a tripwire based on IFM in a setup presented in figure 1.

4. Invisible tripwire

Nevertheless, an IQT is possible. We realize it through a combination of an efficient IFM apparatus and a proper interrogation technique. A possible IQT apparatus is presented in figure 2 and is based on an N-pass IFM apparatus, which offers improved efficiency η due to the quantum Zeno effect [4, 5]. A crucial part of the IQT apparatus is, however, a quantum interrogation technique that deals much better with high sensitivity of the N-pass IFM to photon loss [6], as well as eliminates the dark-port condition. This technique is based on the partial Zeno effect and actually adds a controllable amount of loss to the detection arm by means of a beam splitter with tunable reflectivity. Any attempt to register a photon (that constitutes a tripwire) as well as crossing the path of a photon would immediately engage the quantum Zeno effect, resulting in drastic reduction of the photon loss. This effect will increase the rate at which photons exit the system and trigger the alarm, with a confidence level given by the Chernoff bound.

The N-pass IFM apparatus itself is based on a polarization interferometer that operates in the basis of linear polarizations $|\text{H}\rangle$ and $|\text{V}\rangle$. The path of vertical polarization constitutes a tripwire. The evolution of a photon's polarization state is described by successive multiplication of matrices $\hat{U}(\theta_N)$, $\hat{L}(\lambda)$ and $\hat{O}(h)$ corresponding to polarization rotation by θ_N and loss, λ, of

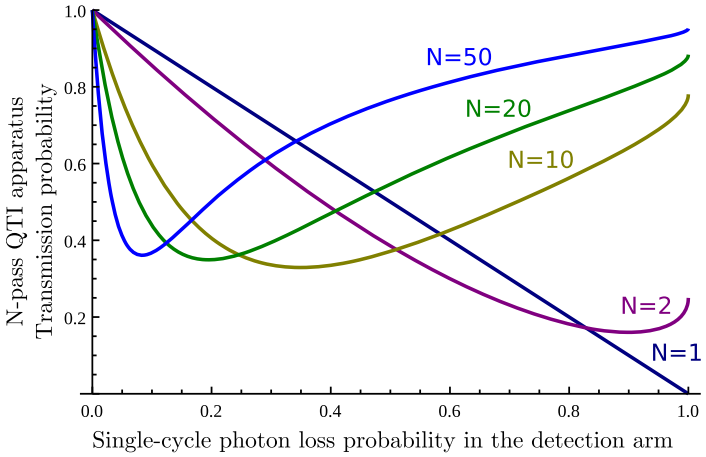

Figure 3. The single-photon transmission probability in an N-pass IQT apparatus P_{tr} for $N\theta_N = \pi/2$ as a function of single-cycle probability of photon loss in the detection arm. Loss in an N-pass IQT is optimized for this partial Zeno effect to take place. The detection of an object is based on increase of transmission.

a photon in the detection arm:

$$\hat{U}(\theta_N) = \begin{bmatrix} \cos\theta_N & -\sin\theta_N \\ \sin\theta_N & \cos\theta_N \end{bmatrix} \quad \text{and} \quad \hat{L}(\lambda) = \begin{bmatrix} 1 & 0 \\ 0 & \sqrt{1-\lambda} \end{bmatrix}, \tag{3}$$

as well as the presence $\hat{O}(h_1) = \hat{L}(1)$ or absence $\hat{O}(h_0) = \hat{L}(0)$ of an object. If the input state of a photon is $|\psi_0\rangle$, then after a single pass it will be $|\psi_1\rangle = \hat{O}(h)\hat{L}\hat{U}(\theta_N)\,|\psi_0\rangle$. The probability of detecting a photon with polarization X after N passes is $P_{\mathrm{X}} = \langle\psi_N|\mathrm{X}\rangle\langle\mathrm{X}|\psi_N\rangle$, while the probability of total transmission is $P_{\mathrm{tr}} = \langle\psi_N|\psi_N\rangle$, where $|\psi_N\rangle$ is obtained by repeating a single-pass evolution N times.

In the IFM apparatus, a photon is initially horizontally polarized, $|\psi_0\rangle = |\mathrm{H}\rangle$. With each pass, polarization is rotated by an angle θ_N, which increases a photon's probability to be in the detection arm, where the photon interacts with a beam splitter before being sent along the tripwire. We present the transmission probability P_{tr} as a function of a single-cycle probability of photon loss in the detection arm, λ, in the absence of an object (see figure 3). P_{tr} is given for a different number of passes but with the same angle of evolution $N\theta_N = \pi/2$. A 100% photon loss corresponds to the presence of an object in the detection arm. One can see that transmission in this case improves with the number of passes due to the quantum Zeno effect. The region of small λ demonstrates how an artificial lossless case behaves since even a small amount leads to a significant drop in the transmission probability. Interestingly, the smallest transmission probability is for relatively high loss, but it is not high enough for the quantum Zeno effect to become apparent. This partial Zeno effect corresponds to a special type of quantum state evolution in the presence of a probabilistic measurement.

Our quantum interrogation technique is based on this special evolution. A controllable amount of loss λ is introduced in the detection arm by means of a beam splitter with tunable reflectivity. This additional loss in the presence of an object reduces the probability of a photon striking the object during a trial, $P_{\mathrm{str}} = (1-\lambda)(1-\cos^{2N}\theta_N)$. Furthermore, we assume that reflectivity and phase shift of the additional beam splitter (inside the interferometer) are

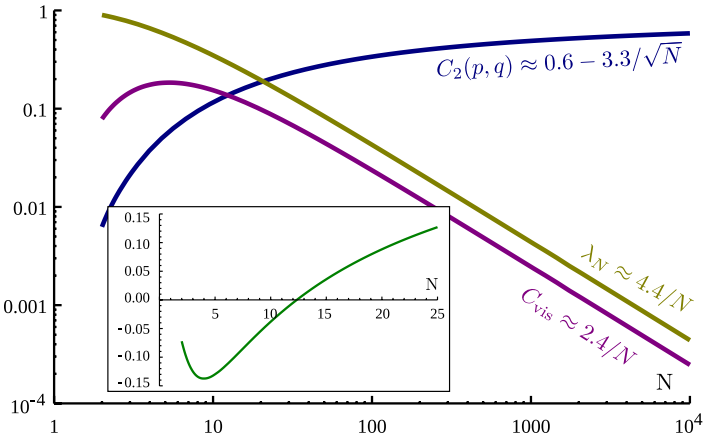

Figure 4. The Chernoff $C_2(p, q)$ and visibility C_{vis} distances as a function of the number of passes N as well as the amount of loss, λ_N, in the detection arm required for partial Zeno to take place. The inset shows a difference between those distances. Invisible detection becomes possible when this difference becomes positive.

constantly adjusted such that detection of a photon at the output is minimal—in order to operate the device at the minimum of the curve shown in figure 3. Such an adjustment is made in order to counteract changes in the environment as well as for the partial Zeno effect to be maintained, which would obviously not be possible in the presence of an object. Thus hypothesis testing is based on two outcomes: a low probability to detect a photon at the output in the absence of an object and 100% in its presence.

The Chernoff distance, in the case of a hypothesis testing apparatus with only two outcomes, registered with probabilities $p_1(1) = p$ and $p_1(2) = \bar{p}$ or $p_0(1) = q$ and $p_0(2) = \bar{q}$, is

$$C_2(p, q) = \xi \ln \frac{\xi}{p} + \bar{\xi} \ln \frac{\bar{\xi}}{\bar{p}}, \tag{4}$$

where $\xi = \ln(\bar{q}/\bar{p})/(\ln(p/\bar{p}) + \ln(\bar{q}/q))$ and $\bar{x} = 1 - x$. Therefore, knowing p and q is sufficient for error estimation. The transmission probability could be calculated analytically only in the presence of the object, $p = \cos^{2N}\theta_N$. However, in the absence of an object, the transmission probability, q, is experimentally available information, which is constantly provided by the IQT apparatus.

There are two primary goals of the IQT apparatus: detection of an object with high certainty, $P_{\text{e}} \to 0$, while staying invisible, $\bar{P}_{\text{vis}}(M) \approx 1$. Although satisfying both goals is, in principle, possible (see figure 4), its success is limited by the number of passages N performed in practice. Thus, the following compromise between confidence level and invisibility is assumed. We would like $\bar{P}_{\text{vis}}(M) > P_{\text{e}}$ (in fact $\bar{P}_{\text{vis}}(M) > P_{\text{e}}^{\max}$), which means a higher likelihood of not hitting the object with a photon than accepting the wrong hypothesis, while maintaining a confidence level above a blind guess: $1 - P_{\text{e}}^{\max} > 0.5$.

5. Results

In our apparatus, it is assumed that a tripwire becomes visible after a single event of a photon striking an object. Therefore, the probability of a tripwire staying invisible after M trials is

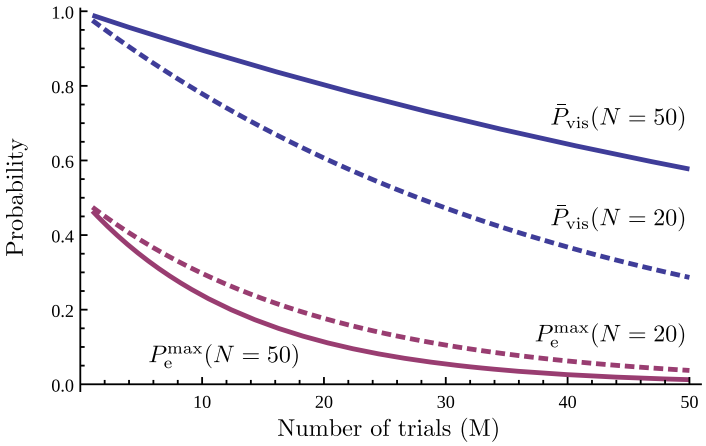

Figure 5. The probability of the tripwire being invisible $\bar{P}_{\rm vis}$ and the maximum error bound $P_{\rm e}^{\rm max}$ are given as functions of the number of trials M, for a given number of passes $N = 20$ and $N = 50$. As N gets larger, $\bar{P}_{\rm vis}$ will stay closer to one, while $P_{\rm e}^{\rm max}$ will go faster to zero.

$\bar{P}_{\rm vis}(M) = \exp(-MC_{\rm vis})$ as before where the visibility distance, $C_{\rm vis} = -\ln(1 - P_{\rm str})$, is defined in terms of the probability of striking an object, as described earlier.

We numerically simulated the performance of the IQT apparatus based on the state evolution described above. For a given number of passes N and θ_N, we numerically found the optimal value of loss λ_N that minimizes the single-trial transmission probability ($P_{\rm tr}$ in the absence of an object). Then we used this value ($\lambda = \lambda_N$) to calculate the Chernoff and visibility distances $C_2(p, q)$ and $C_{\rm vis}$. Figure 4 summarizes these results for a total angle of evolution $N\theta_N = \pi/2$ as a function of the number of passes. This reveals that at least 13 passes are necessary for visibility distance to become smaller than Chernoff distance thus allowing for $\bar{P}_{\rm vis}(M) > 2P_{\rm e}(M)$. While the IQT operating at $N = 100$ is experimentally feasible with current technology, the plots are extended over the range $N > 100$ in order to demonstrate the asymptotic behaviour.

The Chernoff and visibility distances are directly translated to the probability of the tripwire being invisible $\bar{P}_{\rm vis}(M) = \exp(-MC_{\rm vis})$, and the maximum error bound of probability making the wrong decision $P_{\rm e}^{\rm max}(M) = \frac{1}{2}\exp(-MC_2(p, q))$. Figure 5 shows the dependence of $\bar{P}_{\rm vis}$ and $P_{\rm e}^{\rm max}$ on the number of trials M, for given numbers of passes $N = 20$ and $N = 50$. We note that, as the number of passes N gets larger, $\bar{P}_{\rm vis}$ stays closer to one and $P_{\rm e}^{\rm max}$ goes faster to zero—allowing the ideal IQT.

Table 1 presents numerical values of the visibility distance, the ratio of the distances, as well as the operational amount of loss in the detection arm, λ_N. It again shows that at least 13 passes are required before the statistical error starts going to zero faster than the probability of staying invisible. It also shows that the requirement of the total angle of rotation to be $N\theta_N = \pi/2$, which is a requirement for the standard N-pass IFM apparatus, could be dropped. One can actually use θ_N as an additional parameter for the optimization of the IQT apparatus. In the case of $\pi/4$, the visibility distance is shortened by a factor of four. The shorter the distance the more trials are necessary, thus allowing for longer acquisition times (with larger M) and better averaging out of any additional errors acquired in a single trial. In addition, one can see

Table 1. Ratio of the distances, visibility distance, with a corresponding controllable loss for two cases of $N\theta_N$.

	$N\theta_N = \pi/2$			$N\theta_N = \pi/4$		
N	$\frac{C_2(p,q)}{C_{\rm vis}(N)}$	$C_{\rm vis}(N)$	λ	$\frac{C_2(p,q)}{C_{\rm vis}(N)}$	$C_{\rm vis}(N)$	λ
5	0.29	0.184	0.575	0.28	0.057	0.523
10	0.75	0.154	0.349	0.79	0.042	0.314
11	0.85	0.147	0.324	0.92	0.039	0.291
12	0.96	0.140	0.302	1.00	0.038	0.271
13	1.07	0.133	0.282	1.14	0.035	0.253
20	1.91	0.098	0.195	2.08	0.025	0.174
50	6.16	0.045	0.084	6.73	0.011	0.075

that the Chernoff distance actually becomes greater relative to the visibility distance, which signifies that for the same probability of invisibility, statistical error could be made smaller for the $\pi/4$ case than it was possible with a greater total angle of rotation. Finally, the amount of controlled loss in the detection arm is relatively high, which is comforting for practical realizations.

6. Conclusion

In conclusion, we have presented an IQT apparatus that is robust against both loss of photons and random phase accumulations in the detection arm due to a built-in feedback. Interaction-free hypothesis testing in an IQT apparatus allows for stealth operation: detection of an intrusion while being virtually undetectable by an intruder. In addition, our apparatus does not require analysing a photon's polarization state and does not rely on an exact $\pi/2$ rotation, thus allowing for the fine-tuning of the performance. Therefore, such an IQT apparatus holds great promise for practical applications related to security.

Acknowledgments

This work was supported by the Army Research Office, the Boeing Corporation, the Department of Energy, the Foundational Questions Institute, the Intelligence Advance Research Projects Activity and the Northrop-Grumman Corporation.

References

[1] Elitzur A and Vaidman L 1993 *Found. Phys.* **23** 987
[2] Kwiat P, Weinfurter H, Herzog T, Zeilinger A and Kasevich M A 1995 *Phys. Rev. Lett.* **74** 4763
[3] Chernoff H 1952 *Annal. Math. Stat.* **23** 493
[4] Kwiat P, Weinfurter H, Herzog T, Zeilinger A and Kasevich M 1995 *Ann. NY Acad. Sci.* **755** 383
[5] Kwiat P G, White A G, Mitchell J R, Nairz O, Weihs G, Weinfurter H and Zeilinger A 1999 *Phys. Rev. Lett.* **83** 4725
[6] Rudolph T 2000 *Phys. Rev. Lett.* **85** 2925